

The origin of MeV gamma-ray diffuse emission from the inner Galactic region

Naomi Tsuji,^{a,b,*} Yoshiyuki Inoue,^{c,b,d} Hiroki Yoneda,^e Reshmi Mukherjee^f and Hirokazu Odaka^g

^aFaculty of Science, Kanagawa University,

2946 Tsuchiya, Hiratsuka-shi, Kanagawa 259-1293, Japan

^bInterdisciplinary Theoretical & Mathematical Science Program (iTHEMS), RIKEN

2-1 Hirosawa, Wako, Saitama 351-0198, Japan

^cDepartment of Earth and Space Science, Graduate School of Science, Osaka University,

Toyonaka, Osaka 560-0043, Japan

^dKavli Institute for the Physics and Mathematics of the Universe (WPI), UTIAS, The University of Tokyo,

5-1-5 Kashiwanoha, Kashiwa, Chiba 277-8583, Japan

^eNishina Center, RIKEN,

2-1 Hirosawa, Wako, Saitama 351-0198, Japan

^fDepartment of Physics and Astronomy, Barnard College, Columbia University,

New York, NY, 10027, USA

^gDepartment of Physics, The University of Tokyo,

7-3-1 Hongo, Bunkyo, Tokyo 113-0033, Japan

E-mail: ntsuji@kanagawa-u.ac.jp

The origin of the inner Galactic emission, measured by COMPTEL with a flux of $\sim 10^{-2}$ MeV cm⁻² s⁻¹ sr⁻¹ in the 1–30 MeV range, has remained unsettled since its discovery in 1994. We investigate the origin of this emission by taking into account individual sources which are not resolved by COMPTEL and the Galactic diffuse emission. The source contribution is estimated for sources crossmatched between the *Swift*-BAT and *Fermi*-LAT catalogs by interpolating the energy spectra in the hard X-ray and GeV gamma-ray ranges, as well as unmatched sources. This results in a flux of $\sim 20\%$ of the COMPTEL excess. The Galactic diffuse emission is calculated by GALPROP to reconcile the cosmic-ray and gamma-ray spectra with observations by AMS-02, *Voyager*, and *Fermi*-LAT, resulting in a flux of $\sim 30\text{--}80\%$ of the COMPTEL emission. Thus, we show that the COMPTEL emission could be roughly reproduced by a combination of the sources and the Galactic diffuse emission. Furthermore, combined with the extragalactic emission, we construct all-sky images in the MeV gamma-ray range to pinpoint some potential interesting targets for future missions, which would be critical for bridging the “MeV gap” in the spectra of gamma-ray sources.

7th Heidelberg International Symposium on High-Energy Gamma-Ray Astronomy (Gamma2022)

4-8 July 2022

Barcelona, Spain

*Speaker

1. Introduction

The MeV gamma-ray domain is the only unexplored window among recent multiwavelength observations in astrophysics, often referred to as the “MeV gap”. One of the open issues in MeV gamma-ray astrophysics is the origin of diffuse emission from the inner Galactic region. The Imaging Compton Telescope COMPTEL onboard the Compton Gamma-Ray Observatory (CGRO) reported the detection of diffuse emission of $10^{-2} \text{ MeV cm}^{-2} \text{ s}^{-1} \text{ sr}^{-1}$ in 1–30 MeV from the inner Galactic region with $|\ell| \leq 30^\circ$ and $|b| \leq 15^\circ$ [7, 17]. This emission was derived by considering the instrumental background and cosmic gamma-ray background (CGB), thus it would contain Galactic Diffuse Emission (GDE) and unresolved sources. Recently, the inner Galactic diffuse emission has been confirmed by other observations such as *INTEGRAL*-SPI [13] and the electron-tracking Compton camera (ETCC) aboard the balloon mission of SMILE-2+ [18].

The origin of the inner Galactic diffuse emission has been in active debate. If the GDE model to account for the diffuse emission by *Fermi*-LAT [1] is extrapolated to the MeV energy range, there is an apparent excess component (e.g., [15]), which is commonly referred to as the COMPTEL excess. There are several scenarios for reproducing the COMPTEL excess: (1) Individual MeV gamma-ray sources should be taken into consideration. (2) There are non-negligible uncertainties on the model of GDE, since it has a lot of unconstrained parameters (e.g., photon field densities, cosmic ray (CR) source distribution, CR injection spectra, and propagation mechanism). Enhancement of one or more of these parameters can make GDE higher to reach the COMPTEL excess [7]. (3) New populations, such as annihilation or decay of dark matter [6] and/or cascaded gamma rays accompanying cosmic neutrinos [8], might be present.

In this proceeding, we investigate the COMPTEL excess by taking into account MeV gamma-ray sources unresolved by COMPTEL and GDE in Section 2. We also explore all-sky images in the MeV gamma-ray range in Section 3.

2. The inner Galactic diffuse emission in MeV

2.1 MeV gamma-ray sources

Although the previous studies (e.g., [11, 13, 17]) proposed that the COMPTEL excess would be attributed by radiation from individual unresolved sources, the quantitative estimation has not been done yet. We estimate this source contribution from a MeV gamma-ray source catalog in [20], which presented a crossmatching between the 105-month *Swift*-BAT [5] and 10-yr *Fermi*-LAT (4FGL-DR2) [3] catalogs, resulting in 156 point-like and 31 extended crossmatched sources. These crossmatched sources, which are both hard X-ray and GeV gamma-ray emitters, are prominent sources in the MeV gamma-ray sky. Among them, 19 point sources and 14 extended sources are located in the inner Galactic region with $|\ell| \leq 30^\circ$ and $|b| \leq 15^\circ$.

We jointly fit the spectral energy distributions (SEDs) of *Swift*-BAT in 14–195 keV and *Fermi*-LAT in 50 MeV–300 GeV. For the fitting model, we adopt log-parabola or two-component models, depending on the sources. The two-component model is a superposition of the models in the *Swift*-BAT and *Fermi*-LAT catalogs. Based on the best-fit model determined by the minimum χ^2 , we estimate spectra in the MeV gamma-ray energy range, sum up all the spectra of the 33 sources in the inner Galactic region, and divide it by the region size. The result of the accumulated source

spectrum is shown in Figure 1. The contribution of all crossmatched sources to the COMPTEL excess is about 10%. See [21] for details.

Besides the crossmatched sources in [20], there exist many unmatched sources that would have a significant contribution accumulatively. In the region with $|\ell| \leq 30^\circ$ and $|b| \leq 15^\circ$, there are 152 *Swift*-BAT and 708 *Fermi*-LAT sources, where the crossmatched sources are excluded. These unmatched sources (860 in total) would be fainter than 10^{-12} erg cm $^{-2}$ s $^{-1}$ in the MeV energy band since they are not detected by *Swift*-BAT or *Fermi*-LAT, with the sensitivity being approximately 10^{-12} erg cm $^{-2}$ s $^{-1}$. If we assume each unmatched source has a flux of 10^{-12} erg cm $^{-2}$ s $^{-1}$, the accumulative source flux is $\sim 10^{-3}$ MeV cm $^{-2}$ s $^{-1}$ sr $^{-1}$, which should be considered as an upper limit. This upper limit flux of the unmatched sources is roughly comparable to that of the crossmatched sources. Combined with the crossmatched sources, the contribution of the sources is $\sim 20\%$ of the COMPTEL excess (Figure 1).

2.2 Galactic diffuse emission

To evaluate Galactic Diffuse Emission (GDE), we make use of GALPROP (version 54 of WebRun), which is designed to calculate astrophysics of CRs (i.e., propagation and energy loss) and photon emissions in the radio to gamma-ray energy bands [12]. In this proceeding, we use the GDE models in the literature [1, 11], which are developed to be consistent with the CR observations by AMS-02 (and *Voyager*) and the gamma-ray observations by *Fermi*-LAT. A baseline model of $S^2Z^4R^{20}T^{150}C^5$ ¹ is selected as a representative of the models in [1] and referred to as Model 1. From [11], we adopt the DRE (i.e., diffusion and re-acceleration) and DRELowV (modified DRE²) models, hereafter referred to as Model 2 and Model 3, respectively.

Since GDE below ~ 100 MeV is dominated by the inverse Compton (IC) component, the difference in Models 1–3 arises from CR electrons in 0.1–1 GeV. Models 2 and 3 are respectively the highest and lowest with the difference of a factor of a few, and Model 1 is in the middle of them. Although there is such uncertainty on the GDE models, $\gtrsim 30\%$ of the COMPTEL excess is contributed by GDE.

2.3 Results and discussion

Figure 1 compares the COMPTEL data points and our models with the three different models of GDE. We show the spectrum of MeV gamma-ray sources, GDE Models 1–3, and the combined spectra of these two components. It should be noted that this direct comparison did not take into account energy dispersion, which may have a significant effect on the result, as described in the data analysis of *INTEGRAL*-SPI [14]. We find that the combination of GDE and the sources can roughly reproduce the COMPTEL excess: the entire spectrum can be sufficiently explained with Model 2 (Figure 1 upper right), and the lowest and highest energy bins of the COMPTEL data can be reproduced with Model 1 (Figure 1 upper left). Model 3 (Figure 1 lower left) is slightly lower than the COMPTEL excess.

¹This model assumes that the source distribution of CRs is SNRs, the Galactic disk is characterized by the height of $z = 4$ kpc and the galactocentric radius of $R = 20$ kpc, and $T_s = 150$ K and $E(B - V) = 5$ mag cut is adopted for determining the gas-to-dust ratio (see [1] for details).

²DRE model with some modifications on parameters of diffusion and particle injection in order to reproduce the CR measurements [11].

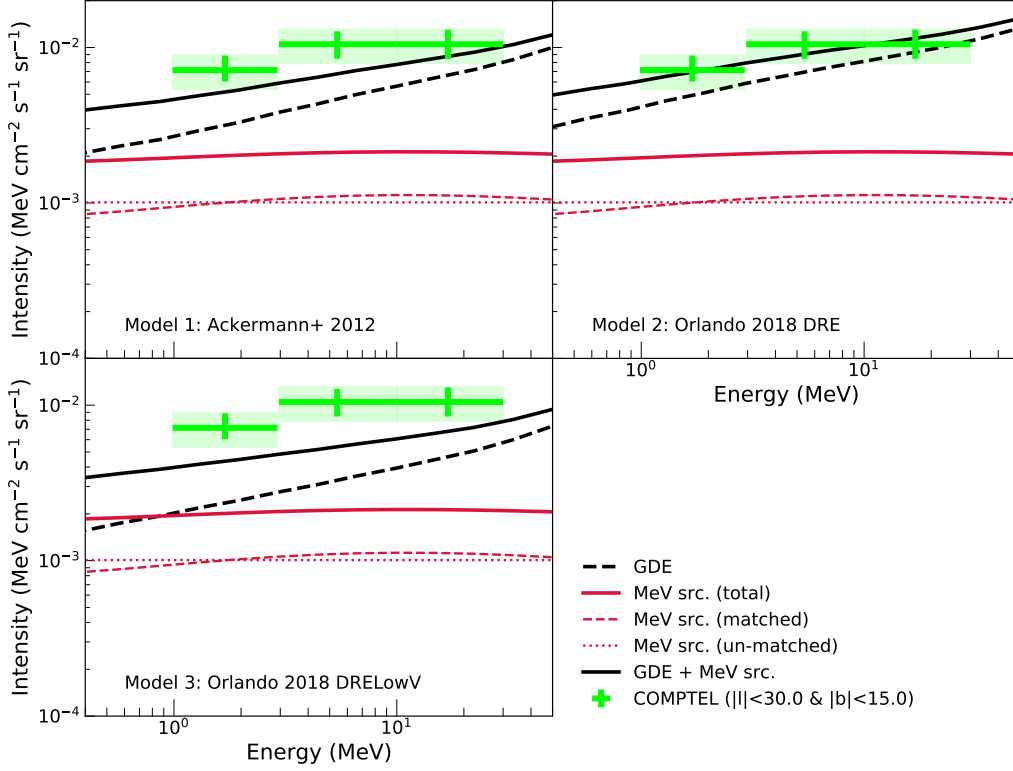


Figure 1: The SEDs of GDE (dashed black line) and the sources (solid red line for all the sources, dashed red for the crossmatched sources, and dotted red for the unmatched sources). The combined spectrum of these two components is illustrated with a solid black line. The results with GDE Models 1, 2, and 3 are respectively shown in the upper left, upper right, and lower left. The COMPTEL emission [7] is indicated by light green points, and light green squares are its systematic error [16].

The spectral shape would provide us with a new constraint. The power-law spectral index is $s \sim -1.9$ ($dN/dE \propto E^s$) for the COMPTEL excess. Figure 1 shows that the spectrum of the accumulated sources is almost flat in the SED with a spectral index of $s \sim -2$. Since the GDE models have $s \sim -1.5$, the MeV gamma-ray sources should play an important role in reproducing the observed spectrum by COMPTEL with $s \sim -1.9$. More precise measurements of the spectrum of each source will enable constraining the accumulative source spectrum, which in turn will be useful to determine the GDE spectrum, especially the index of the primary electrons responsible for the IC radiation.

Since the dominant component in the energy range of the COMPTEL excess is GDE, the uncertainty of GDE prevents us from reaching a robust conclusion. The uncertainty arises from the amount of CR electrons. The CR electrons in 100–1000 MeV, which produce 1–30 MeV photons via IC scattering, are different by a factor of ~ 4 , depending on the models. To distinguish these models is important in the perspective of CR feedback on galaxy evolution: CRs can produce a non-thermal pressure gradient and enhance the degree of ionization in molecular clouds, significantly affecting a star-forming activity (e.g., [10]). The density of the photon fields across the Galaxy is not well constrained, which also makes the GDE model somewhat uncertain in the MeV gamma-ray band.

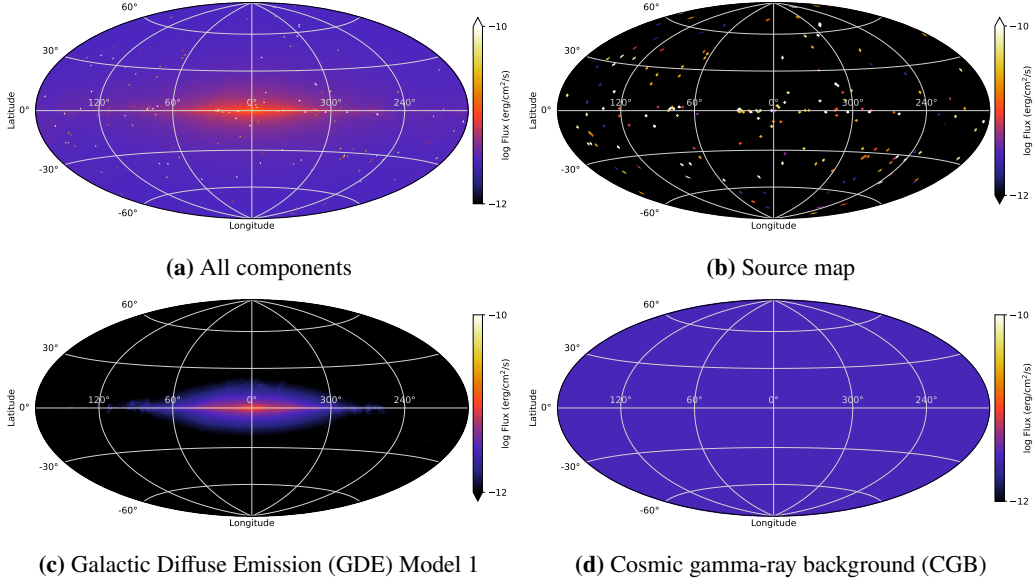


Figure 2: The all-sky maps of the 1–10 MeV flux, shown in the Galactic coordinate and hammer projection.

If we assume that the interstellar radiation field is locally enhanced, such as in the Galactic bulge or a large Galactic CR halo, GDE in the inner Galactic region is increased enough to reach the flux level of the COMPTEL excess [7].

As indicated by Model 3, we would need additional component(s) to reconcile with the COMPTEL emission. Possible explanations are low-mass ($\lesssim 280$ MeV) annihilating dark matter coupling to first-generation quarks [6] and/or cascaded gamma rays accompanying cosmic neutrinos [8], which would open up a new window for these studies.

3. MeV gamma-ray all-sky map

This section presents predicted MeV gamma-ray all-sky maps, which would be useful for observation strategies of future missions. The all-sky map comprises three components: sources, Galactic Diffuse Emission (GDE), and cosmic gamma-ray background (CGB). The source map (Figure 2b) consists of 187 crossmatched sources in [20]. The flux is estimated by fitting the *Swift*-BAT and *Fermi*-LAT SEDs by log-parabola or two-component models, as mentioned in Section 2.1. The extended sources are illustrated as point sources here, but this will be improved in the future work. The GDE map (Figure 2c) makes use of Model 1 [1] described in Section 2.2. For the CGB map (Figure 2d), we assume the spectrum in the literature [22] and the isotropic distribution.

The 1–10 MeV all-sky maps of each component and the total are illustrated in Figure 2. GDE is dominant in the low-latitude sky, while it is dominated by CGB at the higher latitude. The flux of GDE and CGB are respectively 0.18–15 and 3.0 in units of 10^{-12} erg cm^{-2} s^{-1} , and 147 sources have flux larger than these values at each location. Our model predicts that there are 123 and 174 sources with the flux in 1–10 MeV being larger than 10^{-11} and 10^{-12} erg cm^{-2} s^{-1} , respectively. These sources would be good targets for future missions [2, 9, 18, 19].

Data release We provide all of the resources of this study (MeV gamma-ray source catalog, Galdef files of the GDE models, and all-sky FITS files) in <https://tsuji703.github.io/MeV-All-Sky>, which will be updated sometimes.

Acknowledgments

We thank the GRAMS collaboration [2] and the MeV gamma-ray community. N.T. acknowledges support from the Japan Society for the Promotion of Science KAKENHI grant No. 22K14064.

References

- [1] Ackermann, M., Ajello, M., Atwood, W. B., et al. 2012, *ApJ*, 750, 3
- [2] Aramaki, T., Adrian, P. O. H., Karagiorgi, G., & Odaka, H. 2020, *Astroparticle Physics*, 114, 107
- [3] Ballet, J., Burnett, T. H., Digel, S. W., & Lott, B. 2020, arXiv:2005.11208
- [4] Binder, T., Chakraborti, S., Matsumoto, S., & Watanabe, Y. 2022, arXiv:2205.10149
- [5] Bird, A. J., Bazzano, A., Malizia, A., et al. 2016, *ApJ Supplement Series*, 223, 15
- [6] Boddy, K. K., & Kumar, J. 2015, *Physical Review D*, 92, 023533
- [7] Bouchet, L., Strong, A. W., Porter, T. A., et al. 2011, *ApJ*, 739, 29
- [8] Fang, K., Gallagher, J. S., & Halzen, F. 2022, arXiv:2205.03740
- [9] Fleischhack, H., 2021, arXiv:2108.02860
- [10] Hopkins, P. F., Butsky, I. S., Panopoulou, G. V., et al. 2021, arXiv:2109.09762
- [11] Orlando, E. 2018, *MNRAS*, 475, 2724
- [12] Porter, T. A., Jóhannesson, G., & Moskalenko, I. V. 2017, *ApJ*, 846, 67
- [13] Siegert, T., Bertheaud, J., Calore, F., Serpico, P. D., & Weinberger, C. 2022, *A&A* 600, A130
- [14] Strong, A. W., Diehl, R., Haloin, H., et al. 2005, *A&A*, 444, 495
- [15] Strong, A. W., Moskalenko, I. V., & Reimer, O. 2004, *ApJ*, 613, 962
- [16] Strong, A. W., Bennett, K., Bloemen, H., et al. 1994, *A&A*, Vol. 292, p. 82-91
- [17] Strong, A. W., Bennett, K., Bloemen, H., et al. 1996, *A&A Supplement*, v.120, p.381-387
- [18] Takada, A., Takemura, T., Yoshikawa, K., et al. 2022, arXiv:2107.00180
- [19] Tomsick, J. A., Zoglauer, A., Sleator, C., et al. 2019, arXiv:1908.04334
- [20] Tsuji, N., Yoneda, H., Inoue, Y., et al. 2021, *ApJ*, 916, 28
- [21] Tsuji, N., Inoue, Y., Yoneda, H., et al. 2023, *ApJ*, 943, 48
- [22] Weidenspointner, G. 2000, in *AIP Conference Proceedings*, Vol. 510, 467–470